

Fabry–Pérot interferometry with stochastic anyonic sources

Sarthak Girdhar,¹ Edvin G. Idrisov,² and Thomas L. Schmidt³

¹*Department of Physics, University of Basel, Klingelbergstrasse 82, 4056, Basel, Switzerland*

²*Department of Physics, United Arab Emirates University, P.O. Box 15551 Al-Ain, United Arab Emirates*

³*Department of Physics and Materials Science, University of Luxembourg, 1511 Luxembourg, Luxembourg*

We investigate the interference of Laughlin quasiparticles (QPs) in the fractional quantum Hall regime that are stochastically injected into a Fabry–Pérot interferometer. We find that the effective Aharonov–Bohm phase accumulated along the interferometer loop acquires an additional contribution of $\sin(2\pi\lambda)/2$ per QP present on it, where $\pi\lambda$ is the QP exchange phase. This contribution originates from time-domain braiding processes associated with injected QPs passing the interferometer quantum point contacts. In the limit of symmetric QP injection, the tunneling current noise exhibits AB oscillations as a function of the total injected current, providing access to the exchange phase $\pi\lambda$. In the regime of large total injection, we identify a universal Fano factor that displays power-law scaling and a characteristic phase shift reflecting real-space QP braiding along the interferometer edges. These results are relevant for accessing anyonic exchange statistics in mesoscopic interferometers.

I. INTRODUCTION

Fermions and bosons are the fundamental classes of particles distinguished by their exchange statistics. In three dimensions, no other kinds of exchange statistics are possible due to the topology of the underlying space [1]. However, in systems which are effectively two-dimensional, quasiparticles (QPs) with statistics between fermions and bosons can also emerge. These QPs are called anyons [2, 3]. The canonical setup for realizing anyons is a fractional quantum Hall state [4], where as a result of strong electron-electron interactions, they emerge as edge excitations with fractional charge and statistics [5–9]. Recent advancements in hybrid mesoscopic devices have made it possible to study these excitations with unprecedented precision [10–15]. These include the fractional quantum Hall states [16, 17], fractional quantum anomalous Hall states [18–21] and fractional topological insulators [22–25].

Along these lines, quantum point contacts (QPCs) have emerged as especially powerful tools, which let us control and probe electronic channels at the nanoscale [26–30]. By tuning transmission and only selectively allowing interference between these different channels, they can reveal several fundamental quantum properties, from QP exchange statistics to phase coherence and conductance properties of sub-gap states. Although interpreting current-voltage characteristics from these devices is often challenging due to factors such as disorder and electron-phonon interactions [31–39], QPCs can in principle be used to determine the fractional charge and exchange statistics of QPs. This can be done through shot noise measurements, anyonic collision, or interferometer experiments [40, 41], including the Fabry–Pérot, Mach-Zehnder, and Hanbury Brown-Twiss interferometers [42–44].

Notably, recent experimental breakthroughs have enabled the construction of anyonic colliders at both integer ($\nu = 2$) and fractional ($\nu = 1/3$) filling factors [45]. Their measurements of zero-frequency cur-

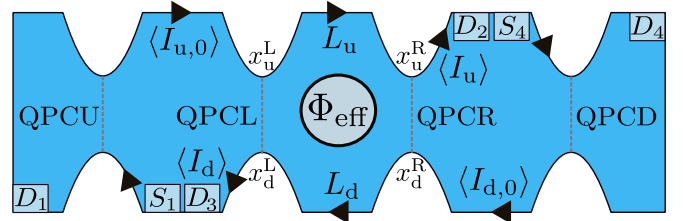


FIG. 1. Schematic of an anyonic Fabry–Pérot interferometer (FPI). The blue region denotes the fractional quantum Hall fluid. Dilute beams of Laughlin quasiparticles (QPs) are injected via the source contacts, QPCU and QPCD, from sources S_1 and S_4 , with average currents $\langle I_{u,0} \rangle$ and $\langle I_{d,0} \rangle$, respectively. The QPs then backscatter and interfere via QPCL and QPCR, forming an interference loop of total perimeter $L_+ = L_u + L_d$, where $L_{u,d}$ are the lengths of the loop arms. Φ_{eff} represents the total effective Aharonov–Bohm phase accumulated upon traversing the loop once. In the nonequilibrium steady state, the outgoing currents $\langle I_u \rangle$ and $\langle I_d \rangle$ are detected at D_2 and D_3 , respectively.

rent cross-correlations and the generalized Fano factor at fractional fillings have demonstrated possible evidence for anyonic exclusion statistics of charge carriers. These findings align with theoretical predictions for the Laughlin state at $\nu = 1/3$ [46]. An essential distinction in this experiment is the use of non-equilibrium source QPCs for individual QP injection, instead of conventional voltage sources [40, 47, 48] which often produce bunched QP flows where ambiguous low-frequency noise measurements obscure the distinction between fractional charges and electrons [49, 50].

Overall, the experimental realization of anyonic colliders and interferometers has sparked numerous investigations in both experimental and theoretical domains [15, 28, 43, 50–63]. Motivated by this progress, in this work we study the interference of Laughlin QPs injected via nonequilibrium source contacts into a Fabry–Pérot interferometer (FPI). Using the nonequilibrium bosonization technique, we calculate the tunneling current, its

noise and the outgoing current cross-correlation. The stochastic nature of the injection process has several interesting effects on the interferometer. In particular, we show that stochastic injection introduces a current-dependent contribution to the effective Aharonov–Bohm (AB) phase arising from time-domain braiding at the interferometer QPCs. This enables pure AB oscillations in the current noise as a function of total injected current (without varying the magnetic field or the system geometry), with a periodicity directly related to the anyonic exchange phase. In the large-injection limit, an effective Fano factor emerges that encodes a characteristic phase shift from real-space QP braiding along the loop arms, offering a robust and dimensionless signature of anyonic statistics.

This paper is organized as follows. In Sec. II, we introduce our model and present a qualitative discussion of the main results, focusing on analogies between an optical and an anyonic FPI, as well as on AB oscillations in the latter. In Sec. III, we describe the model Hamiltonian, the nonequilibrium bosonization technique, and the correlation functions relevant for our setup. Building on this formalism, in Secs. IV and V we compute the tunneling current, its noise, and the outgoing currents’ cross-correlator in the nonequilibrium steady state. In Sec. VI, we analyze AB oscillations in the current noise and discuss signatures of anyonic exchange statistics through a Fano factor. We conclude with a summary and an outlook in Sec. VII.

II. MODEL AND SUMMARY OF THE MAIN RESULTS

Our setup consists of an anyonic FPI in a Hall-bar geometry, as shown in Fig. 1. Dilute beams of Laughlin QPs are injected into the “up” (u) and “down” (d) arms from sources S_1 and S_4 , respectively, via weak backscattering at the source contacts QPCU and QPCD. The corresponding average injected currents are respectively denoted by $\langle I_{u,0} \rangle$ and $\langle I_{d,0} \rangle$. The injected QPs subsequently propagate along the edges and interfere through tunneling at the interferometer QPCs labelled as QPCL and QPCR, forming an interference loop of total perimeter $L_+ = L_u + L_d$. Here, $L_u = x_u^R - x_u^L$ and $L_d = x_d^L - x_d^R$ denote the path lengths along the up and down arms, respectively.

All gates defining the QPCs are operated in the weak pinchoff regime, which is essential for QP tunneling. In the opposite limit of nearly opaque barriers, tunneling occurs only via electrons, precluding access to the exchange properties of fractional QPs [64].

As a QP propagates along the FPI loop, it acquires an AB phase, giving rise to quantum interference effects. In general, this phase depends on the applied magnetic field, the area enclosed by the interferometer loop, and the number of QPs localized within it. The latter can be controlled, for example, by a central gate that selectively de-

pletes charge from the interior of the loop. As we demonstrate below, the total AB phase can also acquire additional contributions due to the injected currents $\langle I_{u,0} \rangle$ and $\langle I_{d,0} \rangle$. This provides a means to probe AB oscillations and anyonic exchange effects without varying the magnetic field or the geometric parameters of the interferometer.

In the nonequilibrium steady state, interference at QPCL and QPCR results in the tunneling of a net current $\langle I_T \rangle$ from edge u to d. The resulting outgoing currents $\langle I_u \rangle$ and $\langle I_d \rangle$ are measured at detectors D_2 and D_3 , respectively.

A. Coherent and incoherent quasiparticle interference

In a classical optical FPI, the sharpest interference fringes are obtained with a monochromatic light source. For a finite spread Δk around a central wave-number k , the visibility of the interference fringes is controlled by the dimensionless product $d \Delta k$, where d denotes the mirror separation. It is therefore instructive to analyze an anyonic FPI from a similar perspective.

We consider the injection of a QP into one of the interferometer arms through a source constriction, from where it propagates toward the tunneling QPCs QPCL and QPCR. In equilibrium, QP–quasihole (QP–QH) pairs are spontaneously generated at both QPCL and QPCR at all times, but owing to electron–hole symmetry, these processes give rise to a zero net current. In the presence of QP injection, however, the situation changes qualitatively. When an injected QP impinges on a QPC, a non-trivial interference arises between processes in which a QP–QH pair is created before and after the arrival of the injected QP at the QPC. This interference corresponds to a braiding process in the time domain [8, 51, 53, 54, 65–67], and results in a statistical phase factor $e^{2\pi i \lambda}$, where $\pi \lambda$ is the QP exchange phase.

For multiple injection events occurring randomly in time with an average injection rate $\langle I_{\alpha,0} \rangle / e^*$ ($\alpha \in \{u, d\}$), where $e^* = e/m$ is the charge of a Laughlin QP, e is the electron charge and m is an odd number, the accumulated statistical phase fluctuates both temporally and spatially along the edge. Since the injection events follow a Poissonian distribution, these fluctuations are characterized by the average rate $\langle I_{\alpha,0} \rangle / e^*$. It is therefore convenient to describe the interferometer in terms of the dimensionless parameters

$$N_u = \frac{L_+ \langle I_{u,0} \rangle}{v e^*}, \quad N_d = \frac{L_+ \langle I_{d,0} \rangle}{v e^*}, \quad (1)$$

where v is the renormalized QP speed along both edges.

Let ζ_L and ζ_R denote the backscattering amplitudes at QPCL and QPCR, respectively. In the limits of both small and large N_u and N_d , the two interferometric QPCs can therefore be effectively replaced by a single QPC with

an effective amplitude ζ_{eff} given by

$$|\zeta_{\text{eff}}|^2 = \begin{cases} |\zeta_L + \zeta_R|^2, & N_{u/d} \ll 1, \\ |\zeta_L|^2 + |\zeta_R|^2, & N_{u/d} \gg 1, \end{cases} \quad (2)$$

corresponding to the coherent and incoherent interference regimes, respectively. In the intermediate regime, $N_{u/d} \sim \mathcal{O}(1)$, one expects damped AB oscillations. This damping arises from the combined effects of the characteristic power-law decay of edge state correlation functions and the dephasing induced by stochastic QP injection processes.

B. Aharonov-Bohm oscillations and fractional exchange statistics

As the injected QPs backscatter at QPCL and QPCR and traverse the FPI loop, they acquire an AB phase in the process. It is generally agreed that this phase has three components [68–70]: a nonuniversal component from backscattering at the QPCs, a contribution determined by the magnetic flux through the loop, and a statistical phase which depends on the filling factor and the total number of QPs in the bulk of the loop. At a constant filling factor, magnetic field and gate voltages responsible for the QPCs, these contributions are essentially constant. It is therefore convenient to incorporate all of these contributions into the relative phase of the tunneling amplitudes at QPCL and QPCR, ζ_l with $l \in \{L, R\}$, according to

$$\zeta_L^* \zeta_R = |\zeta_L| |\zeta_R| e^{i\Phi}. \quad (3)$$

However, in addition to these equilibrium contributions, QP injection at the source contacts also introduces an additional phase component. As discussed above, individual injection events generate random phase fluctuations along the edge. In the nonequilibrium steady state, these fluctuations give rise to an average phase per QP residing on the interferometric arms. Using the nonequilibrium bosonization technique, which is nonperturbative in the injection QPCs, we find this contribution to be $\sin(2\pi\lambda)/2$, leading to an effective phase

$$\Phi_{\text{eff}} = \Phi + \frac{N}{2} \sin(2\pi\lambda) \quad (4)$$

where

$$N = N_u + N_d \quad (5)$$

corresponds to the average total number of injected QPs on the interferometer arms.

We denote the interference contributions to the tunneling current, its zero-frequency noise and the outgoing currents' cross-correlator as $\langle I_{\text{int}} \rangle$, $\langle S_{\text{int}} \rangle$ and $\langle K_{\text{int}} \rangle$, respectively. Under symmetric biasing condition, i.e.,

$I_- = \langle I_{u,0} \rangle - \langle I_{d,0} \rangle = 0$, we find that $\langle S_{\text{int}} \rangle$ exhibits pure AB oscillations as N is varied.

$$\langle S_{\text{int}} \rangle|_{I_- = 0} \propto \cos(\Phi_{\text{eff}}). \quad (6)$$

Importantly, N can be tuned by adjusting the total injected current $I_+ = \langle I_{u,0} \rangle + \langle I_{d,0} \rangle$, while keeping L_+ , e^* , and hence Φ fixed.

Additionally, when two anyons are exchanged along the FPI loop in the presence of the background phase Φ_{eff} , their combined two-body wavefunction picks up the phase $\Phi_{\text{eff}} + \pi\lambda$, where the second term is purely a spatial exchange contribution. We find that this phase shift of $\pi\lambda$ can be observed through an effective Fano factor F , defined as [46]

$$F\left(\frac{I_-}{I_+}, N\right) = \frac{\langle K_{\text{int}} \rangle}{e^* I_+ \frac{\partial}{\partial I_-} \langle I_T \rangle_{\text{int}} \Big|_{I_- = 0}}. \quad (7)$$

In the limit $I_- = 0$ and $N \rightarrow \infty$, this ratio obeys

$$1 - F \propto \frac{\cos(\Phi_{\text{eff}})}{\cos(\Phi_{\text{eff}} + \pi\lambda)}. \quad (8)$$

The phase shift of $\pi\lambda$ appearing in the denominator arises from real-space exchange of QPs along the interferometer arms. Equations (6) and (8) constitute the two central results of this work and, in principle, allow for a direct measurement of the anyonic exchange phase $\pi\lambda$ in the proposed setup.

III. FORMALISM AND APPROACH

A. Bosonization

In order to describe the one-dimensional edges u and d , we use the bosonization technique [71]. For now we employ equilibrium bosonization; the effects of the injection QPCs will be considered in the next subsection. The anyonic field operator $\psi_\alpha(x, t)$ on an edge is

$$\psi_\alpha(x) = \frac{1}{\sqrt{2\pi a}} e^{i\phi_\alpha(x)}, \quad \alpha \in \{u, d\}, \quad (9)$$

where a is a short-distance ultraviolet cutoff. The corresponding QP charge density is

$$\rho_\alpha(x) = \frac{e}{2\pi} \partial_x \phi_\alpha(x). \quad (10)$$

The field $\phi_\alpha(x)$ is a chiral bosonic field satisfying the equal-time commutation relation

$$[\phi_\alpha(x_1), \phi_\beta(x_2)] = i\pi\lambda \delta_{\alpha\beta} \text{sgn}(x_1 - x_2), \quad (11)$$

where $\lambda = 1/m$ for a Laughlin state. In general, edge reconstruction or impurity-induced dephasing may result in $e\lambda \neq e^*$ [72]. However, in the present work we do not

consider these complications. We note that no chirality index appears in the commutation relation in Eq. (11), since the coordinate systems on both edges are defined to increase in the direction of QP propagation. As a result, all modes are effectively right-moving, and a chirality label is unnecessary.

The effective Hamiltonian of the system is written as

$$H = \sum_{\alpha} H_{\alpha} + H_{\text{T}}, \quad (12)$$

where the first term describes free, chiral Laughlin QP modes on edge α and is given by

$$H_{\alpha} = \frac{v}{4\pi\lambda} \int dx [\partial_x \phi_{\alpha}(x)]^2. \quad (13)$$

The second term, H_{T} , describes weak QP tunneling between the upper and lower edges through QPCL and QPCR, and takes the form

$$H_{\text{T}} = \sum_{l \in \{\text{L}, \text{R}\}} (A_l + A_l^{\dagger}), \quad (14)$$

where A_l denotes the operator that transfers a fractional charge e^* from the upper to the lower edge through the l^{th} QPC. Explicitly,

$$A_l = \zeta_l e^{i\phi_{\text{u}}(x_{\text{u}}^l) - i\phi_{\text{d}}(x_{\text{d}}^l)}. \quad (15)$$

It is worth emphasizing that the backscattering amplitudes ζ_l are complex numbers rather than operators. Strictly speaking, locality of the tunneling operators associated with spatially separated QPCs would normally require the introduction of Klein factors in the definition of the QP field operators in Eq. (9), ensuring that $[A_{\text{L}}, A_{\text{R}}] = 0$. However, using the equal-time commutation relation in Eq. (11), one finds that in the absence of Klein factors,

$$A_{\text{L}} A_{\text{R}} = e^{i\pi\lambda[\text{sgn}(x_{\text{u}}^{\text{R}} - x_{\text{u}}^{\text{L}}) + \text{sgn}(x_{\text{d}}^{\text{R}} - x_{\text{d}}^{\text{L}})]} A_{\text{R}} A_{\text{L}}. \quad (16)$$

For a Fabry-Pérot geometry, the sign functions in the exponent of Eq. (16) cancel exactly [73, 74], see Fig. 1, implying that A_{L} and A_{R} commute. The tunneling Hamiltonian in Eq. (14) therefore already satisfies the required locality conditions, and we proceed without introducing Klein factors.

We now go to the interaction picture with H_{T} acting as a perturbation. The bosonic fields evolve as

$$\phi_{\alpha}(x, t) = \phi_{\alpha}(x - vt, 0). \quad (17)$$

Using Eq. (11), we can then write down the time-dependent commutation relation

$$[\phi_{\alpha}(x_1, t_1), \phi_{\beta}(x_2, t_2)] = i\pi\lambda\delta_{\alpha\beta} \text{sgn}[x_1 - x_2 - v(t_1 - t_2)]. \quad (18)$$

When the difference $I_{-} = \langle I_{\text{u},0} \rangle - \langle I_{\text{d},0} \rangle$ is nonzero, the presence of QPCL and QPCR allows a net QP current to

tunnel between the edges u and d. This tunneling current is defined as

$$I_{\text{T}} = ie^*[H_{\text{T}}, N_{\text{d}}] = ie^* \sum_l (A_l^{\dagger} - A_l), \quad (19)$$

where

$$N_{\text{d}}(t) = \int \frac{dx}{2\pi} \partial_x \phi_{\text{d}}(x, t) \quad (20)$$

is the total number of QPs on the lower edge. It satisfies the current conservation equation,

$$\langle I_{\text{T}} \rangle = \langle I_{\text{u},0} \rangle - \langle I_{\text{u}} \rangle = \langle I_{\text{d}} \rangle - \langle I_{\text{d},0} \rangle. \quad (21)$$

B. Nonequilibrium correlation functions

The equilibrium correlation function of the tunneling operators is given by [71]

$$\begin{aligned} \langle A_l(t) A_{l'}^{\dagger}(t') \rangle_{\text{eq.}} &= \zeta_l \zeta_{l'}^* \tau_c^{2\lambda} \frac{e^{-\frac{i\pi\lambda}{2} \text{sgn}(t-t' - (x_{\text{u}}^l - x_{\text{u}}^{l'})/v)}}{|t-t' - (x_{\text{u}}^l - x_{\text{u}}^{l'})/v - i\tau_c|^{\lambda}} \\ &\times \frac{e^{-\frac{i\pi\lambda}{2} \text{sgn}(t-t' - (x_{\text{d}}^l - x_{\text{d}}^{l'})/v)}}{|t-t' - (x_{\text{d}}^l - x_{\text{d}}^{l'})/v + i\tau_c|^{\lambda}}, \end{aligned} \quad (22)$$

where $(l, l') \in \{\text{L}, \text{R}\}$ and $\tau_c \propto a/v$ is a short-time cut-off. The average is taken with respect to the equilibrium ground state at zero temperature [75].

We now incorporate the effect of the source QPCs on these correlation functions. A naive approach based on perturbation theory in the corresponding backscattering amplitudes fails, as such an expansion is known to be divergent [64, 76, 77]. A nonperturbative description of the injection process is therefore required [46, 78, 79].

Consider rare, instantaneous, and Markovian injection of QPs into edge α through a source QPC located at position x_{inj} . For a single injection event occurring at time t_{inj} , the QP charge density undergoes the shift

$$\rho_{\alpha}(x, t_{\text{inj}}) \rightarrow \rho_{\alpha}(x, t_{\text{inj}}) + e^* \delta(x - x_{\text{inj}}). \quad (23)$$

where $\delta(x - x_{\text{inj}})$ denotes the Dirac delta function. Using Eq. (10), this corresponds to a kink in the bosonic field,

$$\phi_{\alpha}(x, t_{\text{inj}}) \rightarrow \phi_{\alpha}(x, t_{\text{inj}}) + 2\pi\lambda \Theta(x - x_{\text{inj}}). \quad (24)$$

For chiral propagation, the corresponding field configuration at arbitrary time t takes the form

$$\phi_{\alpha}(x, t) \rightarrow \phi_{\alpha}(x, t) + 2\pi\lambda \Theta(x - x_{\text{inj}} - v(t - t_{\text{inj}})). \quad (25)$$

Thus, the effect of the source QPCs can be treated non-perturbatively by representing each injected QP as a soliton propagating along the edge. This c-number shift manifests itself in correlation functions as a phase factor.

In particular, the equilibrium correlator in Eq. (22) is modified according to

$$\langle e^{i\phi_\alpha(x,t)} e^{-i\phi_\alpha(x,t')} \rangle \rightarrow \langle e^{i\phi_\alpha(x,t)} e^{-i\phi_\alpha(x,t')} \rangle \times e^{-2\pi i\lambda [\Theta(t-t_0) - \Theta(t'-t_0)]}, \quad (26)$$

where

$$t_0 = t_{\text{inj}} + \frac{x - x_{\text{inj}}}{v} \quad (27)$$

is the arrival time of the injected QP at position x . The correlator thus acquires a phase factor $e^{-2\pi i\lambda \text{sgn}(t-t')}$ if and only if the injected QP crosses the point x between times t and t' , and remains unchanged otherwise. This phase accumulation is the essence of time-domain braiding [8]: the arrival of a QP between t' and t corresponds to a closed loop in time enclosing a statistical flux $2\pi\lambda$.

For multiple injection events occurring independently and following Poissonian statistics, with average rates $\langle I_{\text{u},0} \rangle / e^*$ and $\langle I_{\text{d},0} \rangle / e^*$ on the upper and lower edges, respectively, one performs a statistical average. This yields

$$\langle A_l(t) A_l^\dagger(0) \rangle_0 = \langle A_l(t) A_l^\dagger(0) \rangle_{\text{eq.}} \chi_{\text{u}}(t) \chi_{\text{d}}(t), \quad (28)$$

where the subscript 0 denotes an out-of-equilibrium scenario and $\chi_\alpha(t)$ are the generators of full counting statistics [80–84]. Explicitly,

$$\chi_{\text{u}}(t) = \exp \left[-\frac{\langle I_{\text{u},0} \rangle |t|}{e^*} (1 - e^{-2\pi i\lambda \text{sgn}(t)}) \right], \quad (29)$$

and

$$\chi_{\text{d}}(t) = \exp \left[-\frac{\langle I_{\text{d},0} \rangle |t|}{e^*} (1 - e^{2\pi i\lambda \text{sgn}(t)}) \right]. \quad (30)$$

where we assumed $\langle I_{\text{u},0} \rangle, \langle I_{\text{d},0} \rangle \geq 0$. Similarly, the non-local correlators take the form

$$\langle A_{\text{R}}(t) A_{\text{L}}^\dagger(0) \rangle_0 = \langle A_{\text{R}}(t) A_{\text{L}}^\dagger(0) \rangle_{\text{eq.}} \times \chi_{\text{d}} \left(t + \frac{L_{\text{d}}}{v} \right) \chi_{\text{u}} \left(t - \frac{L_{\text{u}}}{v} \right). \quad (31)$$

Injection events thus introduce stochastic phase shifts in the edge. For Poissonian injection, the variance of these phase fluctuations scales with the mean injection rate, implying that the real part of $\log \chi_\alpha(t)$ leads to exponential dephasing at large currents and long times. The imaginary part, as we show below, gives rise to an effective contribution to the AB phase.

In the nonequilibrium steady state, the main contribution from these correlations comes from large times $|t| \gg e^* / \langle I_{\alpha,0} \rangle$. This is exactly where the injection events can be considered to be Markovian. It must be noted that for this to follow, Eqs. (29) and (30) cannot be used for integer values of λ .

IV. TUNNELING CURRENT

Using the definition of the tunneling current operator in Eq. (19), the expectation value of the tunneling current to leading order in H_{T} is obtained from the Kubo formula,

$$\langle I_{\text{T}} \rangle = e^* \sum_{l,l'} \int dt \langle [A_l^\dagger(0), A_{l'}(t)] \rangle_0 \equiv \sum_{l,l'} \langle I_{ll'} \rangle, \quad (32)$$

where $[,]$ denotes a commutator. It is convenient to decompose this current as

$$\begin{aligned} \langle I_{\text{T}} \rangle &= \langle I_{\text{dir}} \rangle + \langle I_{\text{int}} \rangle, \\ \langle I_{\text{dir}} \rangle &= \langle I_{\text{LL}} \rangle + \langle I_{\text{RR}} \rangle, \\ \langle I_{\text{int}} \rangle &= \langle I_{\text{LR}} \rangle + \langle I_{\text{RL}} \rangle, \end{aligned} \quad (33)$$

where the direct contribution $\langle I_{\text{dir}} \rangle$ arises from tunneling at the individual QPCs, while the interference contribution $\langle I_{\text{int}} \rangle$ encodes the effects of tunneling processes involving both QPCL and QPCR.

We parametrize the injected currents on the upper and lower edges in terms of

$$I_{\pm} = \langle I_{\text{u},0} \rangle \pm \langle I_{\text{d},0} \rangle. \quad (34)$$

The direct tunneling current is then given by (refer to App. A for details)

$$\begin{aligned} \langle I_{\text{dir}} \rangle &= C (|\zeta_{\text{L}}|^2 + |\zeta_{\text{R}}|^2) \Gamma(1 - 2\lambda) (\Omega^2 + \xi^2)^{\lambda - \frac{1}{2}} \\ &\times \sin(\pi\lambda) \sin \left[(1 - 2\lambda) \tan^{-1} \left(\frac{\xi}{\Omega} \right) \right], \end{aligned} \quad (35)$$

where $C = 4\tau_c^{2\lambda} e^*$ and

$$\begin{aligned} \Omega &= \frac{I_+}{e^*} [1 - \cos(2\pi\lambda)], \\ \xi &= \frac{I_-}{e^*} \sin(2\pi\lambda). \end{aligned} \quad (36)$$

The interference contribution takes the form (note that $\langle I_{\text{RL}} \rangle = \langle I_{\text{LR}} \rangle^*$)

$$\begin{aligned} \langle I_{\text{int}} \rangle &= C \left(\frac{L_+}{2v} \right)^{1-2\lambda} |\zeta_{\text{L}}| |\zeta_{\text{R}}| \sin(\pi\lambda) \\ &\times \text{Im} \left\{ e^{i\Phi_{\text{eff}}} \left[e^\mu f(z) - e^{-\mu} f(z^*) \right] \right\}, \end{aligned} \quad (37)$$

where we introduced

$$f(z) = 2^{\frac{1}{2}-\lambda} \pi^{-\frac{1}{2}} \Gamma(1 - \lambda) z^{\lambda - \frac{1}{2}} K_{\frac{1}{2}-\lambda}(z), \quad (38)$$

and $K_\nu(z)$ denotes the modified Bessel function of the second kind. Moreover, we used

$$\mu = \frac{I_- L_+}{2ve^*} [1 - \cos(2\pi\lambda)], \quad z = \frac{L_+}{2v} (\Omega + i\xi). \quad (39)$$

In both currents, we dropped correction terms of order $\tau_c^{2\lambda+1}$, since they vanish in the limit $\tau_c \rightarrow 0$, as expected

from the RG irrelevance of the backscattering operators. We note that the function $f(z)$ is analytic in the open right half of the complex plane. Since $\text{Re}(z) \geq 0$, the fractional powers of z appearing in its definition are free of branch ambiguities. Finally, we note from Eq. (37) that as a result of the injection process, the effective phase around the FPI loop is given by

$$\Phi_{\text{eff}} = \Phi + \frac{N}{2} \sin(2\pi\lambda). \quad (40)$$

This expression can be interpreted in the following way: due to the Poissonian injection process, new QPs enter the FPI loop at time intervals of approximately e^*/I_+ , such that ve^*/I_+ can be interpreted as the average distance between them. The ratio $N = I_+L_+/ve^*$ then corresponds to the average number of QPs on the loop, each contributing an effective phase $\sin(2\pi\lambda)/2$ due to time-domain braiding processes as it backscatters through QPCL and QPCR. By changing the total current injected into the loop, one can thus study pure AB oscillations in the setup. We will elaborate on this in Sec. VI A.

V. CURRENT NOISE AND CROSS-CORRELATIONS

We now turn to the fluctuations of the tunneling current. The zero-frequency noise is given by

$$\langle \delta I_{\text{T}}^2 \rangle_{\omega=0} = (e^*)^2 \sum_{l,l'} \int dt \langle \{A_l^\dagger(0), A_{l'}(t)\} \rangle_0 = \sum_{l,l'} \langle S_{ll'} \rangle, \quad (41)$$

where $\{, \}$ denotes an anticommutator. As before, we decompose the noise into a direct contribution $\langle S_{\text{dir}} \rangle = \langle S_{\text{LL}} \rangle + \langle S_{\text{RR}} \rangle$ and an interference contribution $\langle S_{\text{int}} \rangle = \langle S_{\text{LR}} \rangle + \langle S_{\text{RL}} \rangle$. The direct noise is found to be

$$\langle S_{\text{dir}} \rangle = C' (|\zeta_{\text{L}}|^2 + |\zeta_{\text{R}}|^2) \Gamma(1-2\lambda) (\Omega^2 + \xi^2)^{\lambda-\frac{1}{2}} \times \cos(\pi\lambda) \cos \left[(1-2\lambda) \tan^{-1} \left(\frac{\xi}{\Omega} \right) \right], \quad (42)$$

where $C' = 4(e^*)^2 \tau_c^{2\lambda}$. The interference contribution reads

$$\langle S_{\text{int}} \rangle = C' \left(\frac{L_+}{2v} \right)^{1-2\lambda} |\zeta_{\text{L}}| |\zeta_{\text{R}}| \text{Re} \left\{ e^{i\Phi_{\text{eff}}} \left[\cos(\pi\lambda) \times (e^\mu f(z) + e^{-\mu} f(z^*)) + e^{-\frac{L_+\Omega}{2v}} W(\tilde{z}) \right] \right\}, \quad (43)$$

where

$$\tilde{z} = \frac{L_+}{2v} \left(\frac{I_-}{I_+} \Omega + i\xi \right) \quad (44)$$

and

$$W(\tilde{z}) = \int_{-1}^1 du \frac{e^{u\tilde{z}}}{(1-u^2)^\lambda} \quad (45)$$

$$= \sum_{k=0}^{\infty} \left(\frac{\tilde{z}}{2} \right)^{2k} \frac{\sqrt{\pi} \Gamma(1-\lambda)}{k! \Gamma(k + \frac{3}{2} - \lambda)}. \quad (46)$$

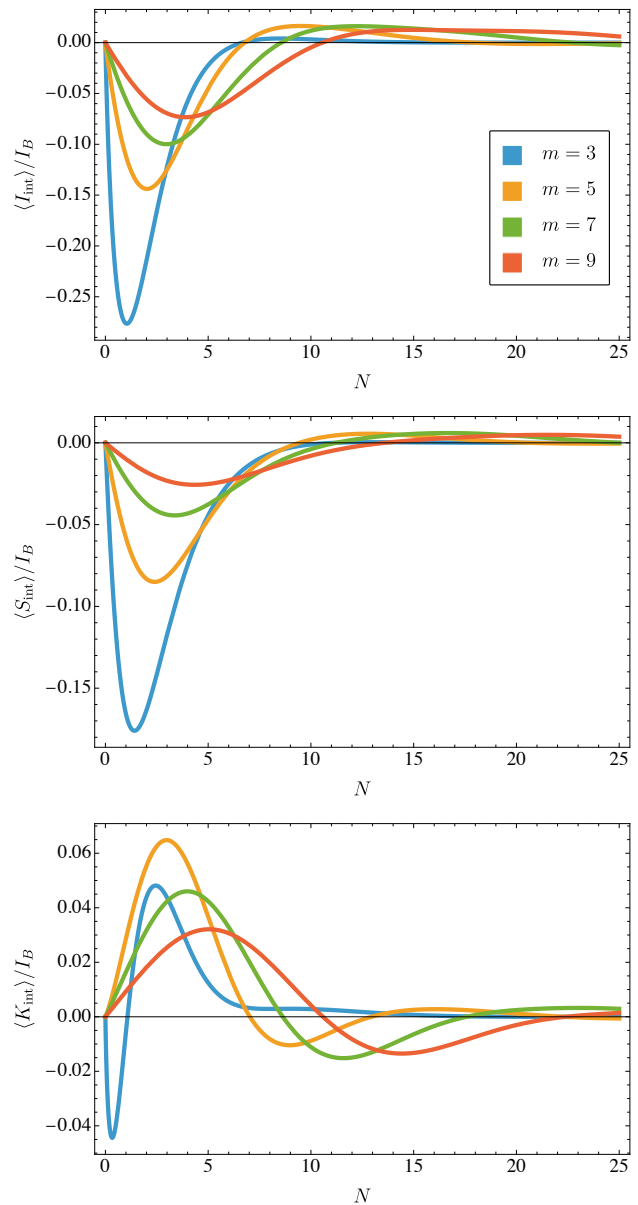


FIG. 2. Interference contributions $\langle I_{\text{int}} \rangle$, $\langle S_{\text{int}} \rangle$, and $\langle K_{\text{int}} \rangle$ to the average tunneling current, its noise, and the outgoing current cross-correlator, shown as functions of $N = I_+L_+/ve^*$ for Laughlin filling fractions $e\lambda = e^* = e/m$. Here, $I_B = |\zeta_{\text{L}}| |\zeta_{\text{R}}| \tau_c^{2\lambda} I_+^{2\lambda-1}$, $I_- = 0.4I_+$ and the bare AB phase $\Phi = \pi/2$. In the large- N limit, interference effects are washed out due to the power-law decay of equilibrium correlation functions and random phase fluctuations along the edges u and d. The quantity I_- captures a phase imbalance between the edges u and d, such that increasing it from zero results in stronger dephasing compared to $I_- = 0$, see Fig. 3.

We now turn to the zero-frequency cross-correlator of the outgoing currents,

$$\langle \delta I_{\text{u}} \delta I_{\text{d}} \rangle_{\omega=0} = \int dt \langle \delta I_{\text{u}}(t) \delta I_{\text{d}}(0) \rangle. \quad (47)$$

Using Eq. (21), the cross-correlator becomes

$$\langle \delta I_u \delta I_d \rangle_{\omega=0} = -\langle \delta I_T^2 \rangle_{\omega=0} + \langle \delta I_{u,0} \delta I_T \rangle - \langle \delta I_T \delta I_{d,0} \rangle. \quad (48)$$

For a Poissonian injection process at the source QPCs, this expression assumes the well-known form [46]

$$\langle \delta I_u \delta I_d \rangle_{\omega=0} = -\langle \delta I_T^2 \rangle_{\omega=0} + e^* \left[\langle I_{u,0} \rangle \frac{\partial}{\partial \langle I_{u,0} \rangle} - \langle I_{d,0} \rangle \frac{\partial}{\partial \langle I_{d,0} \rangle} \right] \langle I_T \rangle. \quad (49)$$

Equation (49) constitutes a nonequilibrium form of a fluctuation–dissipation relation. The first term captures the noise generated at the interferometer QPCs (QPCL and QPCR), while the second term accounts for fluctuations originating from the injected currents $\langle I_{\alpha,0} \rangle$ at the source contacts QPCU and QPCD. As in the case of the tunneling current and its noise, the cross-correlator naturally decomposes into direct and interference contributions. Denoting its interference contribution by $\langle K_{\text{int}} \rangle$, we find

$$\langle K_{\text{int}} \rangle = -\langle S_{\text{int}} \rangle + e^* \left[\langle I_{u,0} \rangle \frac{\partial}{\partial \langle I_{u,0} \rangle} - \langle I_{d,0} \rangle \frac{\partial}{\partial \langle I_{d,0} \rangle} \right] \langle I_{\text{int}} \rangle. \quad (50)$$

The explicit expression for $\langle K_{\text{int}} \rangle$, as well as a derivation of Eq. (49) for our setup, are presented in Apps. B and C, respectively. In the limit $L_+ \rightarrow 0$, we get fully coherent interference. Our results then reduce to those in Ref. [46]. We remark that although the calculations above are carried out explicitly for an interferometer with two QPCs, the resulting expressions for the tunneling current and its noise [see Eqs. (32) and (41)] take the form of sums over pairs of interferometric QPCs. This form allows for a straightforward generalization to an arbitrary number n of interferometer QPCs, which we present in App. D.

We show the dependence of $\langle I_{\text{int}} \rangle$, $\langle S_{\text{int}} \rangle$, and $\langle K_{\text{int}} \rangle$ on N in Fig. 2, all of which exhibit the expected damped oscillatory behavior. As discussed above, this damping originates from the combined effect of the power-law decay of Luttinger-liquid correlation functions and an additional exponential suppression due to QP injection at the source contacts. The oscillations arise from both the effective AB phase Φ_{eff} and the imaginary part of the complex parameter z , see Eq. (39). The latter captures a phase imbalance between QPs injected into the edges u and d , such that increasing the effective bias I_- from zero enhances the randomness of phase fluctuations accumulated along the FPI arms, resulting in stronger dephasing. Consequently, the oscillations in Fig. 2 are not purely AB in origin, but instead encode information about both QP statistics and transport properties. To isolate purely AB oscillations, we therefore set $I_- = 0$, as discussed in the following section.

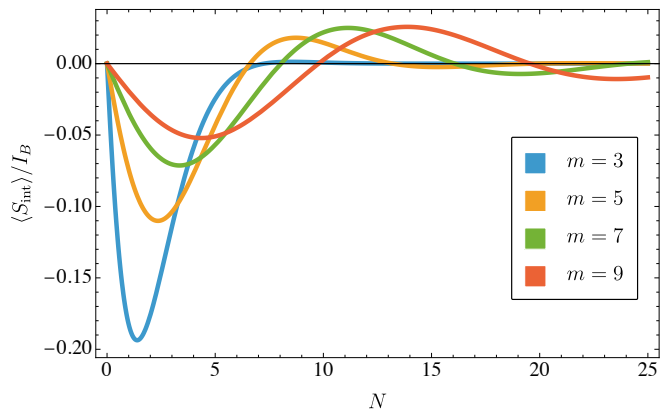


FIG. 3. Aharonov–Bohm (AB) oscillations of the interference contribution to the tunneling current noise, $\langle S_{\text{int}} \rangle$, shown as a function of $N = I_+ L_+ / (v e^*)$ for $e\lambda = e^* = e/m$. The parameters are $I_B = |\zeta_L| |\zeta_R| \tau_c^{2\lambda} I_+^{2\lambda-1}$, $\Phi = \pi/2$, and $I_- = 0$. The oscillation frequency is $\sin(2\pi\lambda)/2$.

VI. AHARONOV-BOHM OSCILLATIONS AND FRACTIONAL STATISTICS

A. Current noise at zero effective bias: $I_- = 0$

In the limit $I_- = 0$, the tunneling current is obviously zero. However, its noise is

$$\langle S_{\text{int}} \rangle |_{I_- = 0} = C' \left(\frac{L_+}{2v} \right)^{1-2\lambda} |\zeta_L| |\zeta_R| \left[2 \cos(\pi\lambda) f \left(\frac{L_+ \Omega}{2v} \right) + W(0) e^{-\frac{L_+ \Omega}{2v}} \right] \cos(\Phi_{\text{eff}}). \quad (51)$$

Equation (51) is one of the two main results of this paper. The zero effective bias current noise corresponds to AB oscillations as a function of N with a constant frequency $\sin(2\pi\lambda)/2$. Therefore, even before the exponential dephasing suppresses all interference effects at $N \gg 1$, they can also be suppressed at the zeroes of the above noise, separated by half-period $2\pi / \sin(2\pi\lambda)$. If an experiment is designed to detect the components of the outgoing currents that change with Φ , the above equation can in principle be used to measure $\pi\lambda$. We show the variation of $\langle S_{\text{int}} \rangle$ against N at $I_- = 0$ in Fig. 3.

We now turn to the second main result, which can help us measure the phase $\pi\lambda$ directly from a spatial QP exchange along the FPI loop.

B. Fano factor

Let us examine the physical origin of the two terms appearing on the right-hand side of Eq. (51). A comparison of Eqs. (37) and (43) shows that the noise, which is defined through an anticommutator, contains an additional contribution arising from the W integral, see Eq. (45). This contribution is absent in the tunneling

current, where it cancels exactly. Such a cancellation is not accidental, but rather a characteristic feature of an FPI.

Indeed, a nonlocal commutator of the form $[A_L^\dagger(0), A_R(t)]$ vanishes within the time window $t \in (-L_d/v, L_u/v)$, as required by locality, see Sec. III A and Eq. (16). Physically, this reflects the fact that such short times are insufficient for QP-QH pairs created at QPCL and QPCR to complete a closed exchange process. Outside this interval, namely for $t \in (-\infty, -L_d/v) \cup (L_u/v, \infty)$, such an exchange process is possible. The corresponding statistical contribution is encoded in the prefactor $\cos(\pi\lambda)$ appearing in Eq. (51), which thus directly reflects the exchange statistics of QP propagation along the FPI arms.

In principle, a statistical phase shift of $\pi\lambda$ in addition to the effective AB phase Φ_{eff} can then be isolated experimentally, as two QPs are exchanged along the FPI loop. To this end, we introduce an effective Fano factor [46, 66], defined as the ratio

$$F\left(\frac{I_-}{I_+}, N\right) = \frac{\langle K_{\text{int}} \rangle}{e^* I_+ \left. \frac{\partial}{\partial I_-} \langle I_T \rangle_{\text{int}} \right|_{I_- = 0}}, \quad (52)$$

where the denominator corresponds to the second term on the right-hand side of Eq. (50) evaluated at $I_- = 0$. By construction, F is dimensionless and therefore independent of microscopic parameters such as the backscattering amplitudes $\zeta_{L,R}$ and the short-time cutoff τ_c . Moreover, this ratio eliminates the exponential fluctuations associated with QP injection at QPCU and QPCD, thereby isolating the contributions arising purely from QP interference along the FPI loop. In the limit $I_- = 0$ and large injection i.e., $N \rightarrow \infty$, the Fano factor reduces to

$$F(0, N \rightarrow \infty) = 1 - \frac{\sqrt{\pi} (N \sin^2(\pi\lambda))^{-\lambda} \cos(\Phi_{\text{eff}})}{2^{1-\lambda} \Gamma(\frac{3}{2} - \lambda) \cos(\Phi_{\text{eff}} + \pi\lambda)}. \quad (53)$$

As discussed, the phase shift of $\pi\lambda$ appearing in the denominator originates from a real-space exchange of QPs along the interferometer arms. Similar to the AB oscillations discussed in Sec. VI A, Eq. (53) thus provides an experimentally accessible signature of the anyonic exchange phase $\pi\lambda$.

VII. CONCLUSION

In this work, we have studied the interference of Laughlin quasiparticles (QPs) injected into a Fabry-Pérot in-

terferometer (FPI) via Poissonian injection at two source contacts. We showed that due to time-domain braiding at the interferometer QPCs, the effective Aharonov-Bohm (AB) phase acquired by the QPs along the FPI loop includes an additional contribution of $\sin(2\pi\lambda)/2$ per QP, where $\pi\lambda$ is the QP exchange phase. For unequal incoming currents, an effective bias produces a net tunneling current between the interferometer arms. We computed the tunneling current, its noise, and the cross-correlator of the outgoing currents, and found that for equal incoming currents, the tunneling current noise exhibits purely AB oscillations as a function of the total number of QPs on the FPI loop, with frequency $\sin(2\pi\lambda)/2$. Moreover, we introduced a Fano factor, a universal, dimensionless quantity that captures the phase shift associated with a QP exchange along the FPI arms. Together, these results provide a simple route to measure the anyonic exchange phase $\pi\lambda$ via noise measurements.

Our model relies on a number of simplifications. We treat the edges as strictly one-dimensional and perfectly chiral, and the injections are assumed to be instantaneous and uncorrelated. Finite edge width, residual interactions, or extended injection pulses could affect the quantitative details of the results [66, 68–70]. Nevertheless, the overall structure of the tunneling current and its fluctuations is expected to remain qualitatively similar, and the framework we present can be adapted to explore more complex filling fractions.

In summary, our study provides a simple setting in which the interplay of injection, interference, and anyonic exchange can be analyzed using both tunneling current and noise as complementary probes of fractional statistics in quantum Hall systems.

ACKNOWLEDGMENTS

We thank Kyrylo Snizhko, Daniel Loss, Jelena Klinovaja and Sumathi Rao for fruitful discussions. S.G. would like to thank the financial support and warm hospitality of the University of Luxembourg where this work was started. E.G.I. acknowledges financial support from the United Arab Emirates University under the Startup Grant No. G00004974, UPAR Grant No. G00005479, AUA-UAEU Grant No. G00005522 and SURE Plus Grant. T.L.S. acknowledges support by the QuantERA grant MAGMA from the National Research Fund Luxembourg under Grant No. INTER/QUANTERA21/16447820/MAGMA.

Appendix A: Derivation of $\langle I_T \rangle$ and $\langle \delta I_T^2 \rangle_{\omega=0}$

We start by calculating the generic contributions $\langle I_{l'l'} \rangle$ and $\langle S_{l'l'} \rangle$, ($l, l' \in \{L, R\}$) to the tunneling current and its noise respectively. We have

$$\langle I_{l'l'} \rangle = e^* \int dt \left\langle \left[A_l^\dagger(0), A_{l'}(t) \right] \right\rangle_0 = e^* \int dt \left(\langle A_l^\dagger(0) A_{l'}(t) \rangle_0 - \langle A_{l'}(t) A_l^\dagger(0) \rangle_0 \right) = e^* (I_1 - I_2) \quad (\text{A1})$$

and

$$\langle S_{l'l'} \rangle = (e^*)^2 \int dt \left\langle \left[A_l^\dagger(0), A_{l'}(t) \right] \right\rangle_0 = (e^*)^2 \int dt \left(\langle A_l^\dagger(0) A_{l'}(t) \rangle_0 + \langle A_{l'}(t) A_l^\dagger(0) \rangle_0 \right) = (e^*)^2 (I_1 + I_2), \quad (\text{A2})$$

where

$$I_1 = \int dt \zeta_L \zeta_L^* \tau_c^{2\lambda} \frac{e^{\frac{i\pi\lambda}{2} [\text{sgn}(t_u) + \text{sgn}(t_d)]}}{|t_u|^\lambda |t_d|^\lambda} \chi_d(t_d) \chi_u(t_u), \quad I_2 = \int dt \zeta_L \zeta_L^* \tau_c^{2\lambda} \frac{e^{-\frac{i\pi\lambda}{2} [\text{sgn}(t_u) + \text{sgn}(t_d)]}}{|t_u|^\lambda |t_d|^\lambda} \chi_d(t_d) \chi_u(t_u), \quad (\text{A3})$$

such that $t_u \equiv t - (x_u^l - x_u^{l'})/v$ and $t_d \equiv t - (x_d^l - x_d^{l'})/v$.

1. Direct terms

The direct terms $\langle I_{\text{dir}} \rangle$ and $\langle S_{\text{dir}} \rangle$ can be calculated when $t_u = t_d = t$. This gives

$$\langle I_{\text{dir}} \rangle = C (|\zeta_L|^2 + |\zeta_R|^2) \int_0^\infty \frac{dt}{t^{2\lambda}} \frac{\sin(\xi t)}{\exp(\Omega t)} = C (|\zeta_L|^2 + |\zeta_R|^2) \Gamma(1-2\lambda) (\Omega^2 + \xi^2)^{\lambda-\frac{1}{2}} \sin(\pi\lambda) \sin \left[(1-2\lambda) \tan^{-1} \left(\frac{\xi}{\Omega} \right) \right], \quad (\text{A4})$$

$$\langle S_{\text{dir}} \rangle = C' (|\zeta_L|^2 + |\zeta_R|^2) \int_0^\infty \frac{dt}{t^{2\lambda}} \frac{\cos(\xi t)}{\exp(\Omega t)} = C' (|\zeta_L|^2 + |\zeta_R|^2) \Gamma(1-2\lambda) (\Omega^2 + \xi^2)^{\lambda-\frac{1}{2}} \cos(\pi\lambda) \cos \left[(1-2\lambda) \tan^{-1} \left(\frac{\xi}{\Omega} \right) \right]. \quad (\text{A5})$$

where Ω and ξ are given by Eq. (36) in the main text.

2. Interference terms

Since $\langle I_{LR} \rangle = \langle I_{RL} \rangle^*$ and $\langle S_{LR} \rangle = \langle S_{RL} \rangle^*$, in the following we only calculate $\langle I_{LR} \rangle$ and $\langle S_{LR} \rangle$. This can be done by setting $t_u = t - L_u/v$ and $t_d = t + L_d/v$ in Eq. (A3). We decompose the integrals I_1 and I_2 into $I_n = I_{n1} + I_{n2} + I_{n3}$, $n \in \{1, 2\}$ such that

$$I_{11} = \int_{L_+/v}^\infty dt \frac{\zeta_R \zeta_L^* \tau_c^{2\lambda} e^{i\pi\lambda}}{(t - L_+/v)^\lambda (t)^\lambda} \chi_d(t) \chi_u(t - L_+/v), \quad (\text{A6})$$

$$I_{12} = \int_0^{L_+/v} dt \frac{\zeta_R \zeta_L^* \tau_c^{2\lambda}}{(-t + L_+/v)^\lambda (t)^\lambda} \chi_d(t) \chi_u(t - L_+/v), \quad (\text{A7})$$

$$I_{13} = \int_0^\infty dt \frac{\zeta_R \zeta_L^* \tau_c^{2\lambda} e^{-i\pi\lambda}}{(t + L_+/v)^\lambda (t)^\lambda} \chi_d(-t) \chi_u(-t - L_+/v), \quad (\text{A8})$$

and $I_{21} = e^{-2\pi i\lambda} I_{11}$, $I_{22} = I_{12}$ and $I_{23} = e^{2\pi i\lambda} I_{13}$. Each of the above three integrals can be calculated as follows.

a. Evaluation of I_{11}

$$I_{11} = \zeta_R \zeta_L^* \tau_c^{2\lambda} e^{i\pi\lambda} \int_{L_+/v}^\infty dt \frac{\exp \left(-\frac{\langle I_{d,0} \rangle t}{e^*} (1 - e^{2\pi i\lambda}) - \frac{\langle I_{u,0} \rangle (t - L_+/v)}{e^*} (1 - e^{-2\pi i\lambda}) \right)}{(t - L_+/v)^\lambda (t)^\lambda}. \quad (\text{A9})$$

Introducing the dimensionless integration variable $u = -1 + (2vt/L_+)$, we get

$$I_{11} = |\zeta_R| |\zeta_L| \tau_c^{2\lambda} e^{i\pi\lambda} \left(\frac{L_+}{2v}\right)^{1-2\lambda} e^{i\Phi_{\text{eff}}} e^\mu f(z), \quad (\text{A10})$$

such that

$$f(z) = \int_1^\infty du \frac{e^{-uz}}{(u-1)^\lambda (u+1)^\lambda} = \frac{2^{\frac{1}{2}-\lambda} z^{\lambda-\frac{1}{2}} \Gamma(1-\lambda) K_{\frac{1}{2}-\lambda}(z)}{\sqrt{\pi}}, \quad (\text{A11})$$

and $K_n(z)$ is the modified Bessel function of the second kind. The parameters Φ_{eff} , μ and z can be read off from Eqs. (39) and (40) in the main text.

b. Evaluation of I_{12}

$$I_{12} = \zeta_R \zeta_L^* \tau_c^{2\lambda} \int_0^{L_+/v} dt \frac{\exp\left(-\frac{\langle I_{d,0} \rangle t}{e^*} (1 - e^{2\pi i \lambda}) + \frac{\langle I_{u,0} \rangle (t - L_+/v)}{e^*} (1 - e^{2\pi i \lambda})\right)}{(-t + L_+/v)^\lambda (t)^\lambda} \chi_d(t) \chi_u(-t + L_+/v). \quad (\text{A12})$$

Again substituting $u = -1 + (2vt/L_+)$ gives

$$I_{12} = |\zeta_R| |\zeta_L| \tau_c^{2\lambda} \left(\frac{L_+}{2v}\right)^{1-2\lambda} e^{i\Phi_{\text{eff}}} e^{-\frac{L_+ \Omega}{2v}} W(\tilde{z}), \quad (\text{A13})$$

where

$$W(\tilde{z}) = \int_{-1}^1 du \frac{e^{-u\tilde{z}}}{(1+u)^\lambda (1-u)^\lambda} = \sum_{k=0}^{\infty} \left(\frac{\tilde{z}}{2}\right)^{2k} \left(\frac{\sqrt{\pi} \Gamma(1-\lambda)}{k! \cdot \Gamma(k + \frac{3}{2} - \lambda)}\right), \quad (\text{A14})$$

and \tilde{z} can be read off from Eq. (44).

c. Evaluation of I_{13}

The third integral is very similar to the first one. We have

$$I_{13} = \zeta_R \zeta_L^* \tau_c^{2\lambda} e^{-i\pi\lambda} \int_0^\infty dt \frac{\exp\left(-\frac{\langle I_{d,0} \rangle t}{e^*} (1 - e^{-2\pi i \lambda}) - \frac{\langle I_{u,0} \rangle (t + L_+/v)}{e^*} (1 - e^{-2\pi i \lambda})\right)}{(t + L_+/v)^\lambda (t)^\lambda}. \quad (\text{A15})$$

After the substitution $u = 1 + (2vt/L_+)$, we get

$$I_{13} = |\zeta_R| |\zeta_L| \tau_c^{2\lambda} e^{-i\pi\lambda} \left(\frac{L_+}{2v}\right)^{1-2\lambda} e^{i\Phi_{\text{eff}}} e^{-\mu} f(z^*). \quad (\text{A16})$$

d. Evaluation of $\langle I_{\text{int}} \rangle$ and $\langle S_{\text{int}} \rangle$

Using Eqs. (A10), (A13) and (A16), we find

$$\langle I_{\text{int}} \rangle = 2e^* \text{Re} (I_{11} - I_{21} + I_{13} - I_{23}) = ((1 - e^{-2\pi i \lambda}) I_{11} + (1 - e^{2\pi i \lambda}) I_{13}), \quad (\text{A17})$$

$$\langle S_{\text{int}} \rangle = 2e^* \text{Re} (I_{11} + I_{21} + 2I_{22} + I_{13} + I_{23}) = ((1 + e^{-2\pi i \lambda}) I_{11} + (1 + e^{2\pi i \lambda}) I_{13} + 2I_{12}). \quad (\text{A18})$$

These equations reduce to the corresponding results in the main text.

Appendix B: Interference terms in cross-correlations $\langle \delta I_u \delta I_d \rangle_{\omega=0}$

Using Eq. (50) from the main text, the interference part of $\langle \delta I_u \delta I_d \rangle_{\omega=0}$ is

$$\langle K_{\text{int}} \rangle = 2\text{Re}(\langle K_{LR} \rangle) = -\langle S_{\text{int}} \rangle + e^* \left(\langle I_{u,0} \rangle \frac{\partial}{\partial \langle I_{u,0} \rangle} - \langle I_{d,0} \rangle \frac{\partial}{\partial \langle I_{d,0} \rangle} \right) \langle I_{\text{int}} \rangle. \quad (\text{B1})$$

We can calculate the derivatives above by differentiating the integrals I_1 and I_2 in App. A under the integral sign. For the sake of brevity, we introduce the notation $\left(\langle I_{u,0} \rangle \frac{\partial}{\partial \langle I_{u,0} \rangle} - \langle I_{d,0} \rangle \frac{\partial}{\partial \langle I_{d,0} \rangle} \right) \equiv \partial$. We find

$$e^* \partial I_{11} = |\zeta_R| |\zeta_L| \tau_c^{2\lambda} e^{i\pi\lambda} \left(\frac{L_+}{2v} \right)^{2-2\lambda} e^{i\Phi_{\text{eff}}} e^\mu \left\{ [\langle I_{d,0} \rangle (1 - e^{2\pi i \lambda})] M_+(z) - [\langle I_{u,0} \rangle (1 - e^{-2\pi i \lambda})] M_-(z) \right\}, \quad (\text{B2})$$

where the integral $M_\pm(z)$ is defined as

$$M_\pm(z) \equiv \int_1^\infty du \frac{(u \pm 1) \exp(-z \cdot u)}{(u+1)^\lambda (u-1)^\lambda} = \frac{2^{1/2-\lambda} \Gamma(1-\lambda)}{\sqrt{\pi}} z^{\lambda-1/2} (K_{\lambda-3/2}(z) \pm K_{\lambda-1/2}(z)). \quad (\text{B3})$$

Similarly, we find

$$e^* \partial I_{13} = |\zeta_R| |\zeta_L| \tau_c^{2\lambda} e^{-i\pi\lambda} \left(\frac{L_+}{2v} \right)^{2-2\lambda} e^{i\Phi_{\text{eff}}} e^\mu \left\{ [\langle I_{d,0} \rangle (1 - e^{-2\pi i \lambda})] M_-(\lambda, z^*) - [\langle I_{u,0} \rangle (1 - e^{2\pi i \lambda})] M_+(\lambda, z^*) \right\}. \quad (\text{B4})$$

Using Eqs. (B2) and (B4),

$$e^* \partial \langle I_{LR} \rangle = 2ie^* \sin(\pi\lambda) |\zeta_R| |\zeta_L| \tau_c^{2\lambda} \left(\frac{L_+}{2v} \right)^{2-2\lambda} e^{i\Phi_{\text{eff}}} \left[e^\mu \left\{ [\langle I_{d,0} \rangle (1 - e^{2\pi i \lambda})] M_+(\lambda, z) - [\langle I_{u,0} \rangle (1 - e^{-2\pi i \lambda})] M_-(\lambda, z) \right\} - e^{-\mu} \left\{ [\langle I_{d,0} \rangle (1 - e^{-2\pi i \lambda})] M_-(\lambda, z^*) - [\langle I_{u,0} \rangle (1 - e^{2\pi i \lambda})] M_+(\lambda, z^*) \right\} \right]. \quad (\text{B5})$$

The above result can be used to calculate $\langle K_{\text{int}} \rangle = -\langle S_{\text{int}} \rangle + 2e^* \text{Re}(\partial \langle I_{LR} \rangle)$.

Appendix C: Derivation of the cross-correlator $\langle \delta I_u \delta I_d \rangle_{\omega=0}$

The cross term $\langle \delta I_T \delta I_{u,0} \rangle_{\omega=0}$ is given by

$$\langle \delta I_T \delta I_{u,0} \rangle_{\omega=0} = \int_{-\infty}^{+\infty} dt \langle I_T(0) \delta I_{u,0}(t) \rangle = -e^* \sum_{l,l'} \int_{-\infty}^{+\infty} dt \int_{-\infty}^0 dt' \langle [A_l(t') + A_l^\dagger(t'), A_{l'}(0) - A_{l'}^\dagger(0)] \delta I_{u,0}(t) \rangle. \quad (\text{C1})$$

Expanding the commutator, we get

$$\langle \delta I_T \delta I_{u,0} \rangle_{\omega=0} = (P_1 + P_2 + P_3 + P_4), \quad (\text{C2})$$

with the four terms given by

$$P_1 = -e^* \sum_{l,l'} \int_{-\infty}^0 dt' \int dt \langle A_l^\dagger(t') A_{l'}(0) \delta I_{u,0}(t) \rangle, \quad P_2 = e^* \sum_{l,l'} \int_{-\infty}^0 dt' \int dt \langle A_{l'}(0) A_l^\dagger(t') \delta I_{u,0}(t) \rangle, \quad (\text{C3})$$

$$P_3 = -e^* \sum_{l,l'} \int_{-\infty}^0 dt' \int dt \langle A_{l'}^\dagger(0) A_l(t') \delta I_{u,0}(t) \rangle, \quad P_4 = e^* \sum_{l,l'} \int_{-\infty}^0 dt' \int dt \langle A_l(t') A_{l'}^\dagger(0) \delta I_{u,0}(t) \rangle.$$

On the other hand, the tunneling current is also given by four terms, see Eq. (21) in the main text.

$$I_T = -e^* \sum_{l,l'} \int_{-\infty}^0 dt' \left(\langle A_l^\dagger(t') A_{l'}(0) \rangle - \langle A_{l'}(0) A_l^\dagger(t') \rangle + \langle A_{l'}^\dagger(0) A_l(t') \rangle - \langle A_l(t') A_{l'}^\dagger(0) \rangle \right), \quad (\text{C4})$$

which we call as $I_{p_1}, I_{p_2}, I_{p_3}$ and I_{p_4} respectively. We now want to write P_1 in terms of the derivative of I_{p_1} with respect to $\langle I_{u,0} \rangle$. We start by introducing the greater Green function

$$iG_d^>(t) = \langle e^{i\phi_d(0,t)} e^{-i\phi_d(0,0)} \rangle. \quad (\text{C5})$$

Writing I_{p_1} in terms of the bosonic fields $\phi_u(x, t)$ and $\phi_d(x, t)$ gives

$$I_{p_1} = -e^* \sum_{l,l'} \zeta_l^* \zeta_{l'} \int_{-\infty}^0 dt' \left[iG_d^> \left(t' - \frac{x_d^l - x_d^{l'}}{v} \right) \right] \langle e^{-i\phi_u(0,t'-x_u^l/v)} e^{i\phi_u(0,-x_{l'}^u/v)} \rangle_{\text{eq.}} \chi_u \left(- \left(t' - \frac{x_l^u - x_{l'}^u}{v} \right) \right). \quad (\text{C6})$$

Under the substitution $t' - (x_u^l - x_u^{l'})/v = \tilde{t}$, we find

$$I_{p_1} = -e^* \sum_{l,l'} \zeta_l^* \zeta_{l'} \int_{-\infty}^{(x_u^{l'} - x_u^l)/v} d\tilde{t} \left[iG_d^> \left(\tilde{t} + \frac{x_u^l - x_u^{l'}}{v} - \frac{x_d^l - x_d^{l'}}{v} \right) \right] \langle e^{-i\phi_u(0,\tilde{t})} e^{i\phi_u(0,0)} \rangle_{\text{eq.}} \chi_u(-\tilde{t}). \quad (\text{C7})$$

Now consider P_1 ,

$$P_1 = -e^* \sum_{l,l'} \int_{-\infty}^0 dt' \left\langle A_l^\dagger(t') A_{l'}(0) \int dt \delta I_{u,0}(t) \right\rangle. \quad (\text{C8})$$

We define $e^* \delta N_{u,0}(t) \equiv \delta I_{u,0}(t) dt$ as the average fluctuations in the injected QP charge via QPCU from time t to $t + dt$. Then the nonequilibrium bosonic field can be decomposed as $\phi_u(x, t) = \phi_u^{\text{eq.}}(x, t) + 2\pi\lambda N_{u,0}(t)$, where $N_{u,0}(t)$ is a ‘‘counting variable’’ with $\langle N_{u,0}(t) \rangle - \langle N_{u,0}(0) \rangle = \langle I_{u,0} \rangle t / e^*$ [see Eq. (24) in the main text] and is uncorrelated with the equilibrium field $\phi_u^{\text{eq.}}$. Using $N_{u,0}(t) = \langle N_{u,0}(t) \rangle + \delta N_{u,0}(t)$, we find

$$P_1 = -e^* \sum_{l,l'} \int_{-\infty}^{(x_u^{l'} - x_u^l)/v} d\tilde{t} \zeta_l^* \zeta_{l'} \left[iG_d^> \left(\tilde{t} + \frac{x_u^l - x_u^{l'}}{v} - \frac{x_d^l - x_d^{l'}}{v} \right) \right] \langle e^{-i\phi_u(0,\tilde{t})} e^{i\phi_u(0,0)} \rangle_{\text{eq.}} \cdot e^* \left\langle e^{-2\pi i \lambda \langle I_{u,0} \rangle \tilde{t} / e^*} e^{2\pi i \lambda [\delta N_{u,0}(-\tilde{t}) - \delta N_{u,0}(0)]} \int_{-\infty}^{+\infty} dt \partial_t \delta N_{u,0}(t) \right\rangle. \quad (\text{C9})$$

where we used $\langle e^{(2\pi i \lambda) (N_{u,0}(-\tilde{t}) - i N_{u,0}(0))} \rangle = \chi_u(-\tilde{t})$. Since the injection events are Markovian, the main contribution to the classical correlation above function will be nonzero only in the interval $t \in (\tilde{t}, 0)$. Its limits can then be truncated as $\int_{-\infty}^{+\infty} \equiv \text{sign}(-\tilde{t}) \int_0^{-\tilde{t}}$, where the sign function preserves the sign of the time step dt when the sign of \tilde{t} changes. This gives us

$$\begin{aligned} P_1 &= -e^* \sum_{l,l'} \int_{-\infty}^{(x_u^{l'} - x_u^l)/v} d\tilde{t} \zeta_l^* \zeta_{l'} \left[iG_d^> \left(\tilde{t} + \frac{x_u^l - x_u^{l'}}{v} - \frac{x_d^l - x_d^{l'}}{v} \right) \right] \langle e^{-i\phi_u(0,\tilde{t})} e^{i\phi_u(0,0)} \rangle_{\text{eq.}} \\ &\quad \times e^* \text{sign}(-\tilde{t}) \left\langle e^{-2\pi i \lambda \langle I_{u,0} \rangle \tilde{t} / e^*} \frac{\partial}{\partial (2\pi i \lambda)} e^{2\pi i \lambda [\delta N_{u,0}(-\tilde{t}) - \delta N_{u,0}(0)]} \right\rangle \\ &= -e^* \sum_{l,l'} \int_{-\infty}^{(x_u^{l'} - x_u^l)/v} d\tilde{t} \zeta_l^* \zeta_{l'} \left[iG_d^> \left(\tilde{t} + \frac{x_u^l - x_u^{l'}}{v} - \frac{x_d^l - x_d^{l'}}{v} \right) \right] \langle e^{-i\phi_u(0,\tilde{t})} e^{i\phi_u(0,0)} \rangle_{\text{eq.}} \\ &\quad \times e^* \text{sign}(-\tilde{t}) \left\langle e^{-2\pi i \lambda \langle I_{u,0} \rangle \tilde{t} / e^*} \frac{\partial}{\partial (2\pi i \lambda)} \left[\chi_u(-\tilde{t}) e^{2\pi i \lambda \langle I_{u,0} \rangle \tilde{t} / e^*} \right] \right\rangle, \end{aligned} \quad (\text{C10})$$

Recalling that

$$\chi_u(t) = \exp \left[-|t| \frac{\langle I_{u,0} \rangle}{e^*} \left(1 - e^{-2\pi i \lambda \text{sgn}(t)} \right) \right], \quad (\text{C11})$$

the above can be rewritten as

$$P_1 = -e^* \langle I_{u,0} \rangle \frac{\partial}{\partial \langle I_{u,0} \rangle} \sum_{l,l'} e^* \zeta_l^* \zeta_{l'} \int_{-\infty}^{(x_u^{l'} - x_u^l)/v} d\tilde{t} \left[iG_d^> \left(\tilde{t} + \frac{x_u^l - x_u^{l'}}{v} - \frac{x_d^l - x_d^{l'}}{v} \right) \right] \langle e^{-i\phi_u(\tilde{t})} e^{i\phi_u(0)} \rangle_{\text{eq.}} \times \chi_u(-\tilde{t}). \quad (\text{C12})$$

Comparing this with Eq. (C7) gives

$$P_1 = e^* \langle I_{u,0} \rangle \frac{\partial}{\partial \langle I_{u,0} \rangle} I_{p_1}. \quad (\text{C13})$$

In this same manner, we can show that

$$P_2 = e^* \langle I_{u,0} \rangle \frac{\partial}{\partial \langle I_{u,0} \rangle} I_{p_2}, \quad P_3 = e^* \langle I_{u,0} \rangle \frac{\partial}{\partial \langle I_{u,0} \rangle} I_{p_3}, \quad P_4 = e^* \langle I_{u,0} \rangle \frac{\partial}{\partial \langle I_{u,0} \rangle} I_{p_4}. \quad (\text{C14})$$

Adding Eqs. (C13) and (C14) gives

$$\langle \delta I_T \delta I_{u,0} \rangle_{\omega=0} = e^* \langle I_{u,0} \rangle \frac{\partial}{\partial \langle I_{u,0} \rangle} \langle I_T \rangle. \quad (\text{C15})$$

Similarly, for the down term, we can show that

$$\langle \delta I_T \delta I_{d,0} \rangle_{\omega=0} = e^* \langle I_{d,0} \rangle \frac{\partial}{\partial \langle I_{d,0} \rangle} \langle I_T \rangle. \quad (\text{C16})$$

Appendix D: Generalization to n QPCs

We assume that the QPCs on the upper (lower) edge are located at positions $x_{u,d}^j$, respectively, with

$$\begin{aligned} x_u^1 &< x_u^2 < \dots < x_u^n, \\ x_d^1 &> x_d^2 > \dots > x_d^n. \end{aligned} \quad (\text{D1})$$

Generalizing the setup in Fig. 1, we allow for QP tunneling with amplitudes ζ_j between positions x_u^j and x_d^j . As discussed in Sec. II in the main text, the limit of vanishing interferometer length, $L_+ \rightarrow 0$, corresponds to fully coherent interference. In this limit, the *direct* tunneling current at a given QPC can be viewed as the *interference* contribution arising from two QPCs separated by distance zero.

With this interpretation, the tunneling current for n QPCs can be written in the form

$$\langle I_T \rangle = C \sum_{j,k=1}^n \sum_{\gamma=\pm 1} \left(\frac{L_+^{jk}}{2v} \right)^{1-2\lambda} |\zeta_j| |\zeta_k| \sin(\pi\lambda) \text{Im} \left\{ e^{i\Phi_{\text{eff}}^{jk} \gamma} e^{\gamma \mu^{jk}} f \left(\frac{L_+^{jk}}{2v} (\Omega + i\gamma\xi) \right) \right\},$$

where $L_+^{jk} = (x_u^j - x_u^k) - (x_d^j - x_d^k)$ denotes the edge length associated with a loop connecting QPCs j and k . The variables Φ_{eff}^{jk} and μ^{jk} are defined analogously,

$$\Phi_{\text{eff}}^{jk} = \Phi^{jk} + \frac{I_+ L_+^{jk}}{2ve^*} \sin(2\pi\lambda), \quad \mu^{jk} = \frac{I_- L_+^{jk}}{2ve^*} [1 - \cos(2\pi\lambda)]. \quad (\text{D2})$$

The corresponding results for $\langle \delta I_T^2 \rangle_{\omega=0}$ and $\langle \delta I_u \delta I_d \rangle_{\omega=0}$ follow in a similar manner.

-
- [1] J. M. Leinaas and J. Myrheim, On the theory of identical particles, *Nuovo Cimento B* **37**, 1 (1977).
[2] F. Wilczek, Quantum mechanics of fractional-spin particles, *Phys. Rev. Lett.* **49**, 957 (1982).
[3] F. Wilczek, Magnetic flux, angular momentum, and statistics, *Phys. Rev. Lett.* **48**, 1144 (1982).
[4] D. C. Tsui, H. L. Stormer, and A. C. Gossard, Two-dimensional magnetotransport in the extreme quantum

- limit, *Phys. Rev. Lett.* **48**, 1559 (1982).
[5] L. Saminadayar, D. C. Glattli, Y. Jin, and B. Etienne, Observation of the $e/3$ fractionally charged Laughlin quasiparticle, *Phys. Rev. Lett.* **79**, 2526 (1997).
[6] R. de Picciotto, M. Reznikov, M. Heiblum, V. Umansky, G. Bunin, and D. Mahalu, Direct observation of a fractional charge, *Nature* **389**, 162 (1997).
[7] M. Carrega, L. Chiroli, S. Heun, and L. Sorba, Anyons

- in quantum Hall interferometry, *Nat. Rev. Phys.* **3**, 698 (2021).
- [8] N. Schiller, Y. Shapira, A. Stern, and Y. Oreg, Anyon statistics through conductance measurements of time-domain interferometry., *Phys. Rev. Lett.* **131** **18**, 186601 (2022).
- [9] V. J. Goldman and B. Su, Resonant tunneling in the quantum Hall regime: Measurement of fractional charge, *Science* **267**, 1010 (1995).
- [10] M. Heiblum and D. E. Feldman, Edge probes of topological order, *Int. J. Mod. Phys. A* **35**, 2030009 (2020).
- [11] A. Das, Y. Ronen, Y. Most, Y. Oreg, M. Heiblum, and H. Shtrikman, Zero-bias peaks and splitting in an Al-InAs nanowire topological superconductor as a signature of Majorana fermions, *Nat. Phys.* **8**, 887 (2012).
- [12] M. Dolev, M. Heiblum, V. Umansky, A. Stern, and D. Mahalu, Observation of a quarter of an electron charge at the $\nu = 5/2$ quantum Hall state, *Nature* **452**, 829 (2008).
- [13] M. Banerjee, M. Heiblum, A. Rosenblatt, Y. Oreg, D. E. Feldman, A. Stern, and V. Umansky, Observed quantization of anyonic heat flow, *Nature* **545**, 75 (2017).
- [14] M. Banerjee, M. Heiblum, V. Umansky, A. Stern, D. Mahalu, and V. Feldman, Observation of half-integer thermal Hall conductance, *Nature* **559**, 205 (2018).
- [15] R. Bhattacharyya, M. Banerjee, M. Heiblum, D. Mahalu, and V. Umansky, Melting of interference in the fractional quantum Hall effect: Appearance of neutral modes, *Phys. Rev. Lett.* **122**, 246801 (2019).
- [16] M. Heiblum and A. Stern, Fractional quantum Hall effects, *Physics World* **13**, 37 (2000).
- [17] Z. F. Ezawa, *Quantum Hall Effects: Recent Theoretical and Experimental Developments*, 3rd ed. (World Scientific, 2013).
- [18] R. B. Laughlin, Anomalous quantum Hall effect: An incompressible quantum fluid with fractionally charged excitations, *Phys. Rev. Lett.* **50**, 1395 (1983).
- [19] E. Spanton, A. Zibrov, H. Zhou, T. Taniguchi, K. Watanabe, M. Zaletel, and A. Young, Observation of fractional Chern insulators in a van der Waals heterostructure, *Science* **360**, 62 (2017).
- [20] F. Xu, Z. Sun, T. Jia, C. Liu, C. Xu, C. Li, Y. Gu, K. Watanabe, T. Taniguchi, B. Tong, J. Jia, Z. Shi, S. Jiang, Y. Zhang, X. Liu, and T. Li, Observation of integer and fractional quantum anomalous Hall effects in twisted bilayer MoTe₂, *Phys. Rev. X* **13**, 031037 (2023).
- [21] N. Nagaosa, J. Sinova, S. Onoda, A. MacDonald, and N. Ong, Anomalous Hall effect, *Rev. Mod. Phys.* **82**, 1539 (2009).
- [22] C. W. Peterson, T. Li, W. Jiang, T. Hughes, and G. Bahl, Trapped fractional charges at bulk defects in topological insulators, *Nature* **589**, 376 (2021).
- [23] W. Zhang, D. Zou, Q. Pei, W. He, J. Bao, H. Sun, and X. Zhang, Experimental observation of higher-order topological anderson insulators., *Phys. Rev. Lett.* **126** **14**, 146802 (2020).
- [24] O. Breunig and Y. Ando, Opportunities in topological insulator devices, *Nat. Rev. Phys.* **4**, 184 (2021).
- [25] J. Maciejko, X.-L. Qi, A. Karch, and S.-C. Zhang, Fractional topological insulators in three dimensions, *Phys. Rev. Lett.* **105**, 246809 (2010).
- [26] C. L. Kane and M. P. A. Fisher, Transmission through barriers and resonant tunneling in an interacting one-dimensional electron gas, *Phys. Rev. B* **46**, 15233 (1992).
- [27] V. Ponomarenko and Y. Lyanda-Geller, Unusual quasiparticles and tunneling conductance in quantum point contacts in $\nu = 2/3$ fractional quantum Hall systems., *Phys. Rev. Lett.* **133** **7**, 076503 (2024).
- [28] J. Nakamura, S. Liang, G. C. Gardner, and M. J. Manfra, Half-integer conductance plateau at the $\nu = 2/3$ fractional quantum Hall state in a quantum point contact, *Phys. Rev. Lett.* **130**, 076205 (2023).
- [29] M. Kiczynski, S. K. Gorman, H. Geng, M. Donnelly, Y. Chung, Y. He, J. Keizer, and M. Simmons, Engineering topological states in atom-based semiconductor quantum dots, *Nature* **606**, 694 (2022).
- [30] J. B. Miller, I. Radu, D. Zumbühl, D. Zumbühl, E. Levenson-Falk, M. Kastner, C. Marcus, L. Pfeiffer, and K. West, Fractional quantum Hall effect in a quantum point contact at filling fraction $5/2$, *Nat. Phys.* **3**, 561 (2007).
- [31] C. L. Kane, M. P. A. Fisher, and J. Polchinski, Randomness at the edge: Theory of quantum Hall transport at filling $\nu=2/3$, *Phys. Rev. Lett.* **72**, 4129 (1994).
- [32] C. L. Kane and M. P. A. Fisher, Impurity scattering and transport of fractional quantum Hall edge states, *Phys. Rev. B* **51**, 13449 (1995).
- [33] A. Mielke, Disorder and the fractional quantum Hall effect: the reduction of the gap, *J. Phys.: Condens. Matter* **2**, 9567 (1990).
- [34] D. F. Mross, Y. Oreg, A. Stern, G. Margalit, and M. Heiblum, Theory of disorder-induced half-integer thermal Hall conductance, *Phys. Rev. Lett.* **121**, 026801 (2018).
- [35] A. V. Shytov, L. S. Levitov, and B. I. Halperin, Tunneling into the edge of a compressible quantum Hall state, *Phys. Rev. Lett.* **80**, 141 (1998).
- [36] G. Finkelstein, P. Glicofridis, S. Tessmer, R. Ashoori, and M. R. Melloch, Imaging of low-compressibility strips in the quantum Hall liquid, *Phys. Rev. B* **61**, R16323 (2000).
- [37] L. S. Levitov, A. V. Shytov, and B. I. Halperin, Effective action of a compressible quantum Hall state edge: Application to tunneling, *Phys. Rev. B* **64**, 075322 (2001).
- [38] E. G. Idrisov, Finite frequency noise in a chiral Luttinger liquid coupled to phonons, *Phys. Rev. B* **100**, 155422 (2019).
- [39] S. Biswas, R. Bhattacharyya, H. K. Kundu, A. Das, M. Heiblum, V. Umansky, M. Goldstein, and Y. Gefen, Shot noise does not always provide the quasiparticle charge, *Nat. Phys.* **18**, 1476 (2022).
- [40] I. P. Levkivskiy, *Mesoscopic Quantum Hall Effect*, 1st ed. (Springer-Verlag Berlin Heidelberg, 2012).
- [41] B. I. Halperin and J. K. Jain, eds., *Fractional Quantum Hall Effects: New Developments* (World Scientific, 2020).
- [42] C. de C. Chamon, D. E. Freed, S. A. Kivelson, S. L. Sondhi, and X. G. Wen, Two point-contact interferometer for quantum Hall systems, *Phys. Rev. B* **55**, 2331 (1997).
- [43] J. Nakamura, S. Liang, G. C. Gardner, and M. J. Manfra, Fabry-Pérot interferometry at the $\nu = 2/5$ fractional quantum Hall state, *Phys. Rev. X* **13**, 041012 (2023).
- [44] T. Werkmeister, J. R. Ehrets, K. Watanabe, T. Taniguchi, B. I. Halperin, A. Yacoby, and P. Kim, Anyon braiding and telegraph noise in a graphene interferometer, *Science* **388**, 730 (2025).
- [45] H. Bartolomei, M. Kumar, R. Bisognin, A. Marguerite, J.-M. Berroir, E. Bocquillon, B. Plaçais, A. Cavanna,

- Q. Dong, U. Gennser, Y. Jin, and G. Fève, *Science* **368**, 173 (2020).
- [46] B. Rosenow, I. P. Levkivskiy, and B. I. Halperin, *Phys. Rev. Lett.* **116**, 156802 (2016).
- [47] E. G. Idrisov, I. P. Levkivskiy, and E. V. Sukhorukov, *Phys. Rev. B* **101**, 245426 (2020).
- [48] E. G. Idrisov, I. P. Levkivskiy, E. V. Sukhorukov, and T. L. Schmidt, Current cross correlations in a quantum Hall collider at filling factor two, *Phys. Rev. B* **106**, 085405 (2022).
- [49] R. Bisognin, H. Bartolomei, M. Kumar, I. Safi, J.-M. Berroir, E. Bocquillon, G. Fève, P. Degiovanni, A. Cavanna, Y. Jin, and G. Fève, Microwave photons emitted by fractionally charged quasiparticles, *Nat. Comm.* **10**, 1708 (2019).
- [50] P. Glidic, O. Maillet, C. Piquard, A. Aassime, A. Cavanna, Y. Jin, U. Gennser, A. Anthore, and F. Pierre, Quasiparticle andreev scattering in the $\nu = 1/3$ fractional quantum Hall regime, *Nat. Comm.* **14**, 514 (2023).
- [51] B. Lee, C. Han, and H.-S. Sim, Negative excess shot noise by anyon braiding, *Phys. Rev. Lett.* **123**, 016803 (2019).
- [52] J.-Y. M. Lee, C. Han, and H.-S. Sim, Fractional mutual statistics on integer quantum Hall edges, *Phys. Rev. Lett.* **125**, 196802 (2020).
- [53] T. Morel, J.-Y. M. Lee, H.-S. Sim, and C. Mora, Fractionalization and anyonic statistics in the integer quantum Hall collider, *Phys. Rev. B* **105**, 075433 (2022).
- [54] C. Mora, Anyonic exchange in a beam splitter (2022), [arXiv:2212.05123](https://arxiv.org/abs/2212.05123).
- [55] J.-Y. M. Lee and H.-S. Sim, Non-abelian anyon collider, *Nat. Comm.* **13**, 6660 (2022).
- [56] J.-Y. M. Lee, C. Hong, T. Alkalay, N. Schiller, V. Umansky, M. Heiblum, Y. Oreg, and H.-S. Sim, Partitioning of diluted anyons reveals their braiding statistics, *Nature* **617**, 277 (2023).
- [57] M. Ruelle, E. Frigerio, J.-M. Berroir, B. Plaçaïs, J. Rech, A. Cavanna, U. Gennser, Y. Jin, and G. Fève, Comparing fractional quantum Hall Laughlin and Jain topological orders with the anyon collider, *Phys. Rev. X* **13**, 011031 (2023).
- [58] H. Bartolomei, M. Kumar, M. Ruelle, and G. Fève, Anyonic and fermionic statistics in a mesoscopic collider, in *Frank Wilczek: 50 Years of Theoretical Physics*, edited by A. J. Niemi, K. K. Phua, and A. Shapere (World Scientific, Singapore, 2022) pp. 11–36.
- [59] J. Nakamura, S. Liang, G. C. Gardner, and M. J. Manfra, Direct observation of anyonic braiding statistics, *Nat. Phys.* **16**, 931 (2020).
- [60] P. Glidic, O. Maillet, A. Aassime, C. Piquard, A. Cavanna, U. Gennser, Y. Jin, A. Anthore, and F. Pierre, Cross-correlation investigation of anyon statistics in the $\nu = 1/3$ and $2/5$ fractional quantum Hall states, *Phys. Rev. X* **13**, 011030 (2023).
- [61] H. K. Kundu, S. Biswas, N. Ofek, V. Umansky, and M. Heiblum, Anyonic interference and braiding phase in a Mach-Zehnder interferometer, *Nat. Phys.* **19**, 515 (2023).
- [62] C. de C. Chamon, D. E. Freed, and X. G. Wen, *Phys. Rev. B* **53**, 4033 (1996).
- [63] E. G. Idrisov and J. Ekström, Quantization of the anyonic spectral density of heat currents, *Phys. Rev. B* **110**, L041402 (2024).
- [64] C. L. Kane and M. P. A. Fisher, Shot noise and the transmission of dilute Laughlin quasiparticles, *Phys. Rev. B* **67**, 045307 (2003).
- [65] B. Rosenow and B. I. Halperin, Braids and beams: Exploring fractional statistics with mesoscopic anyon colliders, [arXiv \(2025\)](https://arxiv.org/abs/2510.04319v2), [arXiv:2510.04319v2](https://arxiv.org/abs/2510.04319v2).
- [66] K. Iyer, F. Ronetti, B. Grémaud, T. Martin, J. Rech, and T. Jonckheere, Finite width of anyons changes their braiding signature, *Phys. Rev. Lett.* **132**, 216601 (2024).
- [67] C. Han, J. Park, Y. Gefen, and H.-S. Sim, Topological vacuum bubbles by anyon braiding, *Nat. Comm.* **7**, 11131 (2016).
- [68] D. E. Feldman and B. I. Halperin, Robustness of quantum Hall interferometry, *Phys. Rev. B* **105**, 165310 (2022).
- [69] B. Rosenow and B. I. Halperin, Influence of interactions on flux and back-gate period of quantum Hall interferometers, *Phys. Rev. Lett.* **98**, 106801 (2007).
- [70] B. I. Halperin, A. Stern, I. Neder, and B. Rosenow, Theory of the fabry-pérot quantum Hall interferometer, *Phys. Rev. B* **83**, 155440 (2011).
- [71] T. Giamarchi, *Quantum Physics in One Dimension* (Clarendon Press, Oxford, 2004).
- [72] B. Rosenow and B. I. Halperin, Nonuniversal behavior of scattering between fractional quantum Hall edges, *Phys. Rev. Lett.* **88**, 096404 (2002).
- [73] I. P. Levkivskiy, A. Boyarsky, J. Fröhlich, and E. V. Sukhorukov, Mach-Zehnder interferometry of fractional quantum Hall edge states, *Phys. Rev. B* **80**, 045319 (2009).
- [74] I. P. Levkivskiy, J. Fröhlich, and E. V. Sukhorukov, Theory of fractional quantum Hall interferometers, *Phys. Rev. B* **86**, 245105 (2012).
- [75] Strictly speaking, the temperature is sufficiently low for the above result to be valid, but still follows $|\zeta_{L,R}| \ll T^{1-\lambda}$ such that a perturbative treatment of the interferometer QPCs remains valid, see Ref. [64].
- [76] I. P. Levkivskiy and E. V. Sukhorukov, Noise-induced phase transition in the electronic Mach-Zehnder interferometer, *Phys. Rev. Lett.* **103**, 036801 (2009).
- [77] I. P. Levkivskiy, Universal nonequilibrium states at the fractional quantum Hall edge, *Phys. Rev. B* **93**, 165427 (2016).
- [78] D. B. Gutman, Y. Gefen, and A. D. Mirlin, *EPL* **90**, 37003 (2010).
- [79] D. B. Gutman, Y. Gefen, and A. D. Mirlin, *Phys. Rev. B* **81**, 085436 (2010).
- [80] D. Kambly, C. Flindt, and M. Buttiker, Factorial cumulants reveal interactions in counting statistics, *Phys. Rev. B* **83**, 1 (2010).
- [81] G. T. Landi, M. J. Kewming, M. T. Mitchison, and P. P. Potts, Current Fluctuations in Open Quantum Systems: Bridging the Gap Between Quantum Continuous Measurements and Full Counting Statistics, *PRX Quantum* **5**, 020201 (2024).
- [82] D. B. Gutman, Y. Gefen, and A. D. Mirlin, Full counting statistics of a Luttinger liquid conductor, *Phys. Rev. Lett.* **105**, 256802 (2010).
- [83] S. Ngo Dinh, D. A. Bagrets, and A. D. Mirlin, Analytically solvable model of an electronic Mach-Zehnder interferometer, *Phys. Rev. B* **87**, 195433 (2013).
- [84] A. Helzel, L. V. Litvin, I. P. Levkivskiy, E. V. Sukhorukov, W. Wegscheider, and C. Strunk, Counting statistics and dephasing transition in an electronic Mach-Zehnder interferometer, *Phys. Rev. B* **91**, 245419 (2015).